

Structural Transformation of Wireframe DNA Origami via DNA Polymerase Assisted Gap-Filling

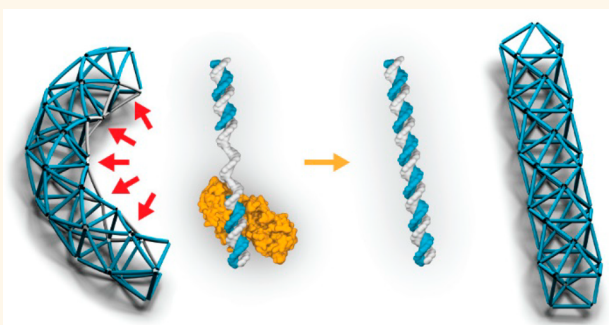
Nayan P. Agarwal,^{#,†} Michael Matthies,^{#,†} Bastian Joffroy,[†] and Thorsten L. Schmidt^{*,†,‡,§,||}

[†]Center for Advancing Electronics Dresden (cfaed), Faculty of Chemistry and Food Chemistry, and [‡]B CUBE—Center for Molecular Bioengineering, Technische Universität Dresden, Dresden, 01062, Germany

 Supporting Information

ABSTRACT: The programmability of DNA enables constructing nanostructures with almost any arbitrary shape, which can be decorated with many functional materials. Moreover, dynamic structures can be realized such as molecular motors and walkers. In this work, we have explored the possibility to synthesize the complementary sequences to single-stranded gap regions in the DNA origami scaffold cost effectively by a DNA polymerase rather than by a DNA synthesizer. For this purpose, four different wireframe DNA origami structures were designed to have single-stranded gap regions. This reduced the number of staple strands needed to determine the shape and size of the final structure after gap filling. For this, several DNA polymerases and single-stranded binding (SSB) proteins were tested, with T4 DNA polymerase being the best fit. The structures could be folded in as little as 6 min, and the subsequent optimized gap-filling reaction was completed in less than 3 min. The introduction of flexible gap regions results in fully collapsed or partially bent structures due to entropic spring effects. Finally, we demonstrated structural transformations of such deformed wireframe DNA origami structures with DNA polymerases including the expansion of collapsed structures and the straightening of curved tubes. We anticipate that this approach will become a powerful tool to build DNA wireframe structures more material-efficiently, and to quickly prototype and test new wireframe designs that can be expanded, rigidified, or mechanically switched. Mechanical force generation and structural transitions will enable applications in structural DNA nanotechnology, plasmonics, or single-molecule biophysics.

KEYWORDS: structural DNA nanotechnology, DNA origami, DNA polymerases, gap-filling, actuation



DNA nanotechnology utilizes a bottom-up, self-assembly approach wherein DNA is assembled into well-defined complex higher-order structures with the help of the specificity of Watson–Crick and Hoogsteen base-pair interactions.^{1–4} The “DNA origami” technique is a particularly robust and popular method to design and build DNA-based nanostructures.^{5–8} This method uses several short DNA oligonucleotides (staple strands) as building blocks along with a long single-stranded DNA as a scaffold-strand. DNA origami structures can be compact and designed with mostly parallel helices. Examples include most flat origami structures⁵ and 3-dimensional structures.^{6,9,10} Alternatively, grid-iron¹¹ or wireframe structures^{12–16} can be designed strictly from triangulated double-stranded helices¹⁵ or where edges consist of no more than two helices.^{13,14,16} The wireframe building principle is more material-efficient, allowing the structure to cover a larger area or encompass a larger volume, and increases the sterical accessibility of the individual DNA helices. Moreover, the structures are stable in a wide range of salt

conditions due to the reduced electrostatic repulsion between the DNA helices. Overall, these examples demonstrate that DNA is a versatile material for constructing shapes. The addressability of DNA origami structures further allows for a complex nanomaterial assembly,¹⁷ with applications ranging from nanophotonics and nanoelectronics to biophysics, nanomedicine, and molecular biology.^{8,18,19}

Apart from building static structures, DNA can also be used to design dynamic molecular motors, walkers, robots, and tweezers, reconfigurable DNA devices such as a DNA origami actuator that can perform autonomous internal motions.^{20,21} The working principle of these examples is often a strand-displacement mechanism. Alternative approaches to build dynamic structures using DNA include temperature or salt

Received: November 24, 2017

Accepted: February 16, 2018

Published: February 16, 2018

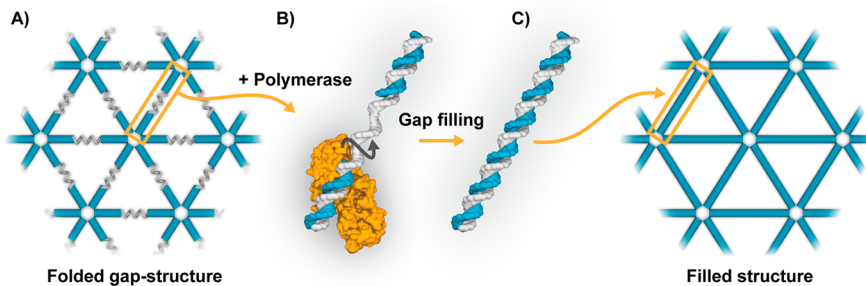


Figure 1. DNA polymerase-assisted gap filling of wireframe DNA origami structures. (A) DNA origami structures are folded such that some or all edges contain unpaired single-strand “gap regions” in the scaffold strand (gray). (B) These flexible gap regions are filled with a polymerase such as T4 DNA polymerase using the staple strands as primers resulting in stiff, double-stranded edges (C). Artistic representations were produced from PDB models of DNA (created using 3DNA)²⁷ and the T4 DNA polymerase (PDB: 1NOY).²⁸

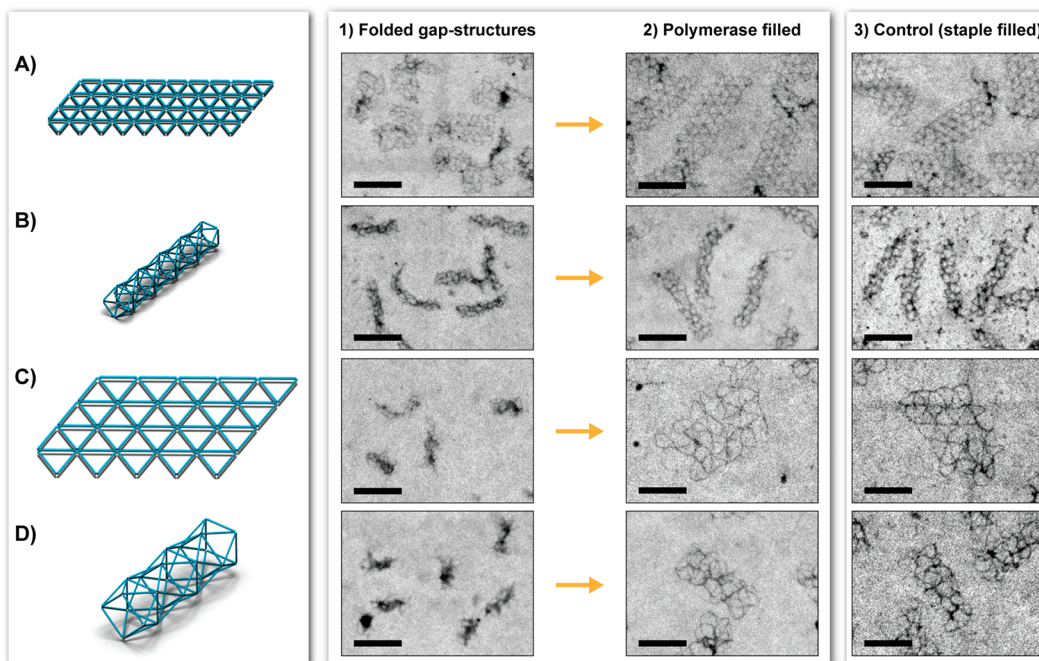


Figure 2. Wireframe DNA structures before and after gap filling. Four structures, (A) flat small, (b) tube small, (c) flat large, and (d) tube large were used here. Artistic models are displayed to scale such that the relative sizes can be compared. The structures containing the gap regions were folded (1). Then T4 DNA polymerase and dNTPs were added to fill the gap regions (2) with the optimized protocol. Enzymatically filled structures are compared with the control structures (3), where the structures were folded with additional staples complementary to the gap regions. Scale bars of tSEM micrographs: 100 nm (wide-field images: Supporting Figures 5–8).

control, restriction enzymes, and the pH, ion,²² or light²³ responsive DNA motives.⁸ Such molecular motors chemically convert energy to induce structural transformations.

A major drawback of prototyping and improving complex DNA nanoscale structures is the cost of DNA oligonucleotides.²⁴ To this end, the usage of staple strand sequences can be minimized by custom scaffolds.²⁵ The drawback is the loss of unique addressability. Alternatively, a polymerase-assisted gap filling process on the M13 scaffold along with Rec A protein was shown to increase the persistence length of double-stranded DNA.²⁶ However, it was concluded that this approach displayed defects when the DNA origami was prefolded and the M13 scaffold was gap-filled as a second step.

In this paper, we have used DNA polymerases to fill designed single-stranded gap regions in DNA origami triangulated truss structures (Figure 1) and to transform the chemical energy

obtained by the DNA polymerases into forces capable of mechanically transforming the structures.

RESULTS AND DISCUSSION

Design of the Structures. To develop a method for a DNA polymerase-assisted gap-filling, four wireframe DNA origami designs were chosen: flat small (FS), tube small (TS), flat large (FL), and tube large (TL). “Small” designs have a typical gap size of 16 or 21 nucleotides (nt) and an edge length of 58 or 63 base pairs (bp) after gap filling, whereas “large designs” typically have gaps of 81 or 86 nt and an edge length of 123 or 128 bp after extension. Similar to our previous work,¹⁵ the flat designs (FS and FL) were modified by exchanging the edge staple strands (orange oligonucleotides in the Supporting Figures 1 and 2) to form the tube designs (TS and TL), which consist of adjacent decahedral units. The resulting tube structures correspond to the 4(0, 1, 1) notation

by Erickson.²⁹ We chose isosceles triangles with two equal legs of odd helical half turns of DNA (58 bp and 123 bp for the small and large designs, respectively) while the base of the triangle consisted of even helical half turns of DNA (63 bp and 128 bp for the small and large designs, respectively). The benefit of this composition of the structures is a planar and relaxed design¹⁴ compared to the design with equilateral triangles with odd helical half turns of DNA in our previous work.¹⁵ The neighboring vertices of the triangles are connected by single-stranded spacers of two nucleotides, for both the scaffold and staple strands. The staple oligonucleotides throughout the design have two domains of 21 bp each that connect the edges of the neighboring triangles, with the exception of the edge oligonucleotides (orange oligonucleotides in the Supporting Figures 1 and 2) that have only one domain of 21 bp. The gap regions are positioned in the middle of each edge of the triangle; for the small designs (FS and TS) these gap regions are 16 and 21 nt long, while for the large designs (FL and TL) they are 79 and 84 nt long. Thus, 33% of the scaffold remains single-stranded for the small design or 66% in the large design. Detailed information for all the designs is in the [cadnano files](#), and [Supporting Figures 1 and 2](#).

Folding of Gap-Structures. The four different wireframe DNA origami structures were self-assembled by slowly annealing the staple strand sets with their respective scaffold strands (p7560 for small designs and p8064 for large designs). The gap-structures and control structures, where the gap regions were filled with additional staples, formed a single product band that migrated slower than the corresponding scaffold strand band in the agarose gel electrophoresis (AGE) analysis ([Supporting Figure 4](#)). The gap regions in the designs did not lead to an aggregation, and the product yield for all the gap structures was calculated to be nearly 90%. This demonstrated the robustness of the wireframe design and supported the possibility of using fewer staples to assemble a structure. The shape of the gap-structures is, however, not well-defined ([Figure 2](#), [Supporting Figures 5–8](#)) as expected due to the high flexibility of single-stranded DNA.

Single-Stranded DNA Binding Proteins. In nature, single-stranded DNA (ssDNA) is produced during strand breaks, replication, recombination, or DNA repair. Single-stranded regions are typically stabilized either by the replication of the counter strand by DNA polymerases or are covered with single-stranded binding (SSB) proteins. Initially, we tested the stabilization of single-stranded gaps with two SSB proteins. SSB proteins have been successfully used for TEM imaging as contrast agents, as they can efficiently highlight the ssDNA regions,³⁰ and we expected a similar behavior. Moreover, RecA and T4 gene 32 protein both exhibit a strong affinity toward ssDNA and are known to stabilize the ssDNA domains and effectively denature potential secondary structures. We therefore explored SSB proteins alone and as an additive for a polymerase-based gap filling. In both cases, SSBs did, however, lead to aggregation, and no defined structures or extension products were observed by native AGE, denaturing PAGE, and tSEM imaging. For these reasons, SSBs were not further investigated (data and more detailed discussion, [Supporting Figure 9](#)).

Gap Filling with Different Polymerases. Next, a purely DNA polymerase-assisted gap filling without SSB proteins was explored with different polymerases including T4 DNA polymerase, DNA polymerase I, Phi29 polymerase, T7 DNA polymerase, Vent DNA polymerase, Taq DNA polymerase,

Phusion high-fidelity DNA polymerase, large Klenow fragment, and Q5 high-fidelity DNA polymerase. For this, the test structure (FS) was incubated with these DNA polymerases in separate vials in the respective buffers provided by the suppliers for 1 h. From all these polymerases, only T4 DNA polymerase is commonly used for gap-filling reactions in biology,³¹ for example in cloning applications.³² To test T4 DNA polymerase extensively, three different incubation temperatures (12, 25, and 37 °C) were tested. On AGE, the product bands of all the three reactions were observed to migrate slower than the control gap structure ([Supporting Figure 10A](#)), indicating an extension by the DNA polymerases.

For all reactions, we further analyzed the extended strands by denaturing PAGE to investigate the extension of the individual staple strands ([Supporting Figure 10](#)). For the control gap FS structure before extension, only distinct 21-mer and 44-mer bands can be observed. After extension with the T4 DNA polymerase, 60-mer and 65-mer bands were observed as expected. An additional continuous smear below the 60-mer band was also observed indicating the formation of shorter undesired side products or incomplete extension. We hypothesized that these products were formed as a result of an increased 3' → 5' exonuclease activity of the DNA polymerase with long incubation times (see below).

The product bands for DNA polymerase I, phi29 polymerase, and large Klenow fragment migrate slower compared to the T4 DNA polymerase product. For DNA polymerase I, this can be explained by the strong 5'-3' exonuclease activity of the polymerase, which presumably digests downstream staple strands leading to the formation of double-stranded (ds) scaffold strands. The Phi29 polymerase and the large Klenow fragment are known for their strong strand-displacement activity resulting in a circular ds M13 and a long ssDNA concatemer and no defined staple bands were observed in the PAGE gels.

Vent DNA polymerase, Taq DNA polymerase, Phusion high-fidelity DNA polymerase, and Q5 high-fidelity DNA polymerase are widely used DNA polymerases for PCR reactions and are typically used at high temperatures. Despite their thermophilic character, gap-filling resulted in a band pattern similar to that of T4 at moderate temperatures (37 °C), both for in AGE and PAGE gels. Furthermore, tSEM micrographs show the formation of defined FS structures ([Supporting Figures 10 and 11](#)) that were comparable to the control structures where the gap regions were filled by complementary staple strands ([Supporting Figure 5](#)).

From all the tested DNA polymerases, Phusion seemed to perform the best for the flat small structures in the first experiments. For the other designs (TS, FL, and TL), product bands with an expected shift were observed in AGE, but PAGE revealed that staple extension did not occur correctly and that the extended structures did not resemble the desired shape in tSEM micrographs except for the flat small structures. We concluded, that extension by Phusion DNA polymerase is not consistent across all designs ([Supporting Figures 12 and 13](#)).

Inactivation of Polymerase. Because of the inconsistent results with Phusion polymerase and since T4 DNA polymerase is widely used for gap-filling in molecular biology, we further optimized conditions for T4 DNA polymerase. We hypothesized that strong 3' → 5' exonuclease activity may have led to the undesired products in the smear on PAGE ([Supporting Figure 10](#)) discussed above. By adding 2-mercaptoproethanol, the enzyme and probably also the exonuclease activity could be

denatured in less than 1 min. This fast quenching provides the necessary control over the reaction time (Supporting Figure 14). The mechanism is not clear, but after the inactivation step, much fewer undesired products were observed and the structures looked more intact in TEM images (Figure 3 and

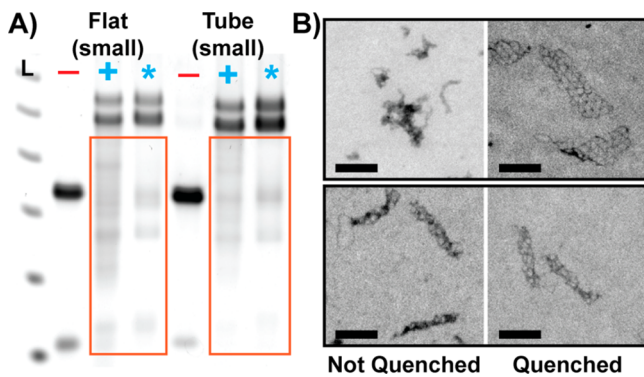


Figure 3. Inactivation of T4 DNA polymerase with 2-mercaptoethanol. (A) PAGE gel analysis to compare the effect of quenching of the polymerase. The lanes marked with a red line (−) contain the structures with the gap regions, while the lanes marked with a blue plus sign (+) contain the enzymatically extended structures without the quenching step and the lanes marked with the asterisk (*) contain the extended structures that were quenched with 2-mercaptoethanol. Samples without the quenching show undesired side products visible as a smear. (B) TEM micrographs of (top) flat small; (bottom) tube small structures, comparing the outcome with and without the inactivation step. Scale bars = 100 nm. More information is in Supporting Figure 14.

Supporting Figure 15). Additionally, the products were comparable to the ones obtained after the gap-filling reaction with Phusion DNA polymerase, with the advantage that the method was now consistent across all the designs. We therefore strongly recommend inactivation of the polymerase after the extension reaction.

Secondary Structures. Next, we tested gap-filling reactions at different temperatures. AGE, PAGE, and tSEM results (Supporting Figures 16 and 17) imply that 25 °C is the optimal reaction temperature for the FS structure, while the reaction time should be restricted to a maximum of 10 min. For the FL structure, fewer low-molecular weight side products were obtained at 37 °C after 3–10 min incubation compared to lower temperatures. Insufficient processivity does not seem to be responsible for temperature-dependent differences, as even after 3 min at 12 °C, the majority of staples were extended to the full-length product and even a 33-fold longer incubation time did not reduce the remaining shorter side products (Supporting Figure 16) significantly. So, even at lower temperatures, the enzyme should in principle be fast enough to extend the gaps. We therefore hypothesize that the additional lower molecular weight bands might be caused by hairpins, which could act as a roadblock to the polymerase. Alternatively, hairpins may also lead to replication slippage,³³ which is an effect inversely related to the DNA polymerase strand-displacement mechanism and would also result in shorter extension products. Much fewer short side products were observed at 37 °C, which would be consistent with the model of hairpins. The higher temperatures would lead to an increased temporary melting (fraying), which could enable the polymerase to successfully read through the hairpin. We observed a similar effect for Phi 29 polymerase which has a high

strand displacement capacity and which had a significantly higher amplification rate if temporary melting (fraying) probabilities were increased due to geometrical constraints.³⁴

To locate potential hairpins, we performed a Gibbs free energy simulation using mfold³⁵ on all the gap regions at four different temperatures (12, 25, 37, and 40 °C) for the two gap designs (small and large). A lower (more negative) Gibbs free energy directly corresponded to stronger hairpin regions (Supporting Figure 18). Increasing the extension temperature to 37 °C eliminated most side products. Alternatively, additional staples complementary to strong hairpins or artificially designed scaffold strands³⁶ with reduced secondary structures may improve extension results for regions with strong secondary structures further.

In conclusion, the optimal conditions for the T4 DNA polymerase assisted gap-filling method are 25 °C for 5 min for the FS and TS structures and 40 °C for 5 min for the FL and TL structures, followed by an inactivation step with 2-mercaptoethanol (Figure 2, Figure 4, and Supporting Figure 4).

Folding Kinetics of Gap Origami. We tested four different protocols (tables in Supporting Figure 19) to find the minimum time needed to fold the gap structures. We tested cooling ramps over 16 h, 1 h, and 10 min, and a 6 min isothermal reaction similar to the one described by Sobczak *et*

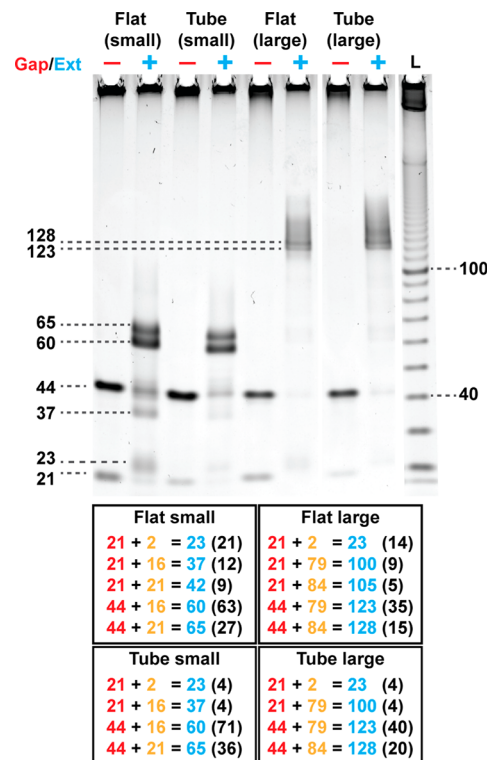


Figure 4. Denaturing PAGE analysis of the DNA polymerase assisted gap filling of the wireframe DNA structures. The lanes marked with a red line (−) contain the structures with the gap regions, while the lanes marked with a blue plus sign (+) contain the enzymatically extended structures. The expected staple strand bands are marked with a dotted line in each lane. The lengths before (red) and after gap filling (blue) and the number of strands for each expected final length is summarized in the inset tables. The occurrence number of each staple extension is denoted in brackets in black. Structures before and after enzymatic extensions were purified by AGE.

al.³⁷ after which the gap structures were extended at the optimized conditions. AGE, PAGE, and AFM results indicated that all the annealing protocols work with comparable efficiency (Supporting Figure 19) and we conclude that despite the utilization of an incomplete staple set the gap structures can be folded in just 6 min and then gap-filled with T4 DNA polymerase in 3 min, resulting in a total reaction time of just 9 min.

Bending of Tubes. Finally, TS structures were folded with gap regions only at one side of the tube (Figure 5A, red arrows,

demonstrate a well-defined structural transformation in DNA origami structures by gap filling polymerases. Varying the number and the position of the gap regions may allow a precise control of the resulting transformation.

CONCLUSIONS

In this paper, we have demonstrated the structural transformations of DNA origami structures induced by strand extension reactions with DNA polymerases. For this purpose, we tested a wide range of DNA polymerases and found that T4 DNA polymerase is the most suitable. The presence of single-stranded gap regions in the design requires fewer staple strands (33% less in small design and 66% less in large design) and allows very fast annealing times in only 6 min compared to 16 h used for most DNA origami structures. Gap regions in the structures act as entropic springs that lead to a collapse of the entire structure if gap regions are introduced on all edges. When gap regions are only introduced on one side of the tubular DNA origami, the resulting structures were selectively curved. The DNA polymerase assisted gap-filling transformed collapsed structures into full-size filled structures or straightens curved structure tubes. In one of our typical reactions, we used 1 μ L of dNTPs (~0.06 €) and 1 μ L of T4 Polymerase (~1 €) to modify 0.4 pmole of DNA origami. We envision that this approach will enable reducing costs for the prototyping of different wireframe origami designs or be used to construct force generating mechanical units which can be switched within 3 min. This switching can, for example, be used to switch plasmonic devices or to build dynamic devices for single-molecule force spectroscopy. The costs of the polymerase could be reduced by 1–2 orders of magnitude when produced in house, which would make this technique attractive for larger scale reactions as well.

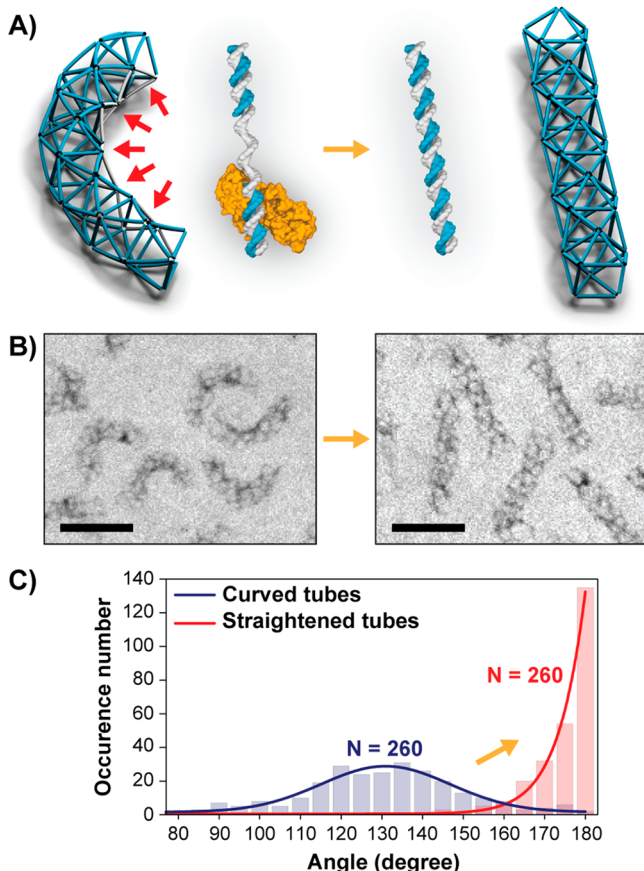


Figure 5. Structural transformation of the wireframe tubes using the DNA polymerase-assisted gap-filling method. Tube small structures were folded with gap regions highlighted by red arrows (A). These gap regions act as entropic springs that force the entire structure to curve. After filling the gap regions with T4 DNA polymerase, tubes were straightened (A-right). (B) tSEM micrographs of the corresponding curved and straightened tubes (scale bars: 100 nm). (C) Histograms of the angular distributions plotted against the occurrence number in respective samples ($N = 260$ for each state). The histograms were fitted with a Gaussian curve with a standard deviation of $130^\circ \pm 15^\circ$ for the curved tubes and $180^\circ \pm 6^\circ$ for the straightened tubes.

Supporting Figure 20), which act as entropic springs and induce a global curvature.³⁸ After filling the gap regions with a polymerase, they were rigidified, thus releasing the bending stresses resulting in a straight tube (Figure 5A right). To quantify the curvature of the tubes, angles were measured from the tSEM micrographs (Supporting Figures 21 and 22), plotted in a histogram (Figure 5) and fitted with a Gaussian curve. The curved tubes had an angle of $130^\circ \pm 15^\circ$, whereas straightened tubes were almost perfectly linear $180^\circ \pm 6^\circ$. These results

MATERIAL AND METHODS

DNA Origami Folding. For folding wireframe DNA origami structures (with or without gap regions) the following mixture composition was used: 20 nM of p8064 (for large design) or p7560 (for small design) scaffold (Tilbit), staple strands set (Eurofins) (sequences in Supporting Information) at 200 nM (each), 1X of NEB 2.1 buffer (New England Biolabs Inc.) that consists of 50 mM NaCl, 10 mM Tris-HCl, 10 mM MgCl₂, and 100 μ g/mL BSA adjusted to pH 7.9. The mixture was annealed in a thermal cycler (Bio-Rad C1000 Touch) from 80 to 65 °C at a rate of $-1\text{ }^\circ\text{C}/\text{min}$ and from 65 °C to room temperature at a rate of $-1\text{ }^\circ\text{C}/\text{min}$ per 20 min. Excess staple strands were then removed by agarose gel electrophoresis. For fast folding the following variations were made to the annealing protocol: 1-h protocol, 1 min at 80 °C, 80 to 65 °C at a rate of $-1\text{ }^\circ\text{C}/20\text{ s}$ and from 65 °C to room temperature at a rate of $-1\text{ }^\circ\text{C}/\text{min}$; 10 min protocol, 1 min at 80 °C followed by cooling down to 20 °C at the rate of $5\text{ }^\circ\text{C}/\text{min}$; 6 min protocol (isothermal), 1 min at 80 and 55 °C for 5 min. Following the annealing reaction, the samples were stored at $-20\text{ }^\circ\text{C}$ in 1.5 mL of DNA LoBind vials (Eppendorf).

Gap Filling of the Wireframe DNA Origami Structures. For the extension of the gap regions the following routes were explored.

SSB Protein-Assisted Gap Filling Method (RecA and T4 gene 32). A 10 μ L sample of 20 nM unpurified gap structures (FS) were added to a 200 μ L PCR tube. To that, the respective SSB protein buffer provided by the supplier was added to a final 1X concentration. Ultrapure water was added to bring the volume of the mixture to 19 μ L. To this mixture 1 μ L of the SSB protein (RecA or T4 gene 32, New England Biolabs) was added and mixed carefully (final volume, 20 μ L). The mixture was incubated for 1 h at 25 °C (for Rec A) or 37 °C (for T4 gene 32). The reacted sample was then used for further analysis and purification by AGE.

Combination of the SSB Protein and T4 DNA Polymerase (RecA +T4 DNA pol; T4 gene 32+T4 DNA pol). A 10 μ L sample of 20 nM unpurified gap structures (FS) was added to a 200 μ L PCR tube. To that, the respective SSB protein buffer provided by the supplier to a final 1X concentration. Ultrapure water was added to bring the volume of the mixture to 18 μ L. To this mixture 1 μ L of each component was added and mixed carefully. Final volume: 20 μ L. The mixture was incubated for 1 h at 25 °C (for Rec A) or 37 °C (for T4 gene 32). The reacted sample was then used for further analysis and purification by AGE.

Initial Test with Different DNA Polymerase-Assisted Gap Filling Methods (T4, T7, DNA pol1, Vent, Taq, Phusion, Q5, Klenow and phi29). A 10 μ L sample of 20 nM unpurified gap structures (FS) were added to a 200 μ L PCR tube. To that, the respective enzyme buffer provided by the supplier was added to a final 1X concentration. Ultrapure water was added to bring the volume of the mixture to 19 μ L. To this mixture 1 μ L of the DNA polymerase was added and mixed carefully. Final volume: 20 μ L. The mixture was incubated for 1 h at 12 °C (for T4) or 25 °C (for T4, DNA pol1) or 30 °C (for phi29) or 37 °C (for T4, T7, Vent, Taq, Phusion, Q5 and Klenow). The reacted sample was then used for further analysis and purification by AGE.

NOTE: All the different activities of the DNA polymerases that are summarized in the main text were derived from the Web site of the supplier (New England Biolabs Inc.).

Final Optimized T4 DNA Polymerase-Assisted Gap Filling Method with 2-Mercaptoethanol Inactivation. A 10 μ L sample of 20 nM unpurified gap structures (FS, TS, FL, and TL) were added to a 200 μ L PCR tube. To that, the respective enzyme buffer was added to bring the final concentration of the buffer to 1X. Ultrapure water was added to bring the volume of the mixture to 17 μ L. To this mixture 1 μ L of the T4 DNA polymerase was added and mixed carefully. The mixture was incubated for 5 min at 25 °C (for FS and TS) or 40 °C (for FL and TL). To stop the reaction, 2 μ L of 2-mercaptoethanol was added and incubated for 1 min at 25 °C. The reacted sample was then used for further analysis and purification by AGE.

NOTE: For all the optimization reactions, the same reaction mixture composition was prepared as described in the initial test section.

Agarose Gel Electrophoresis. For the AGE analysis, 1% agarose gels (DNA pure grade, VWR) was cast with 0.5X TBE buffer supplemented with 12 mM MgCl₂ and 1X Gelgreen nucleic acid gel stain (Biotium). TBE buffer (0.5X) with 12 mM MgCl₂ was used as a running buffer. A 15 μ L aliquot of sample solution was mixed with 3 μ L of 6X gel loading dye (50% glycerol, 5 mM Tris, 1 mM EDTA (pH 8.0), 12 mM MgCl₂, 0.25% bromophenol blue, and 0.25% of xylene cyanol). Electrophoresis was performed at 70 V for 2 h at room temperature. As a reference, 10 μ L of 1 kb plus DNA ladder (Thermo Scientific) were added. The gel was imaged with a Typhoon FLA 9500 gel scanner (GE Healthcare) using the excitation wavelength of 473 nm suitable for SYBR safe stained gels.

For the purification of the wireframe DNA origami structures (with or without gap regions), the desired band was cut out with a razor blade, and the excess agarose was carefully removed. The slice was then chopped, transferred into a DNA gel extraction column (Bio-Rad, Freeze'n Squeeze) and centrifuged at 4800 rcf, at room temperature for 5 min. After centrifugation, the inner filter tube was rotated by 180° and centrifuged again under same conditions to completely filter out the sample from the agarose debris. The purified sample was transferred into a DNA LoBind tube and stored at 4 °C.

PAGE Gel Analysis. Casting 15% Denaturing PAGE Gel. An 18.2 g of urea (99.5% for analysis, ACROS Organics) were dissolved in 20 mL of ultrapure water. To the mixture, the following components were added: 5 mL of 10X Tris-EDTA-Borate (TBE) buffer, 18.75 mL of acrylamide/bis(acrylamide) (29:1); 40% solution (Alfa Aesar), 400 μ L of freshly dissolved ammonium persulfate, 10% wt (AppliChem), 30 μ L of N,N,N',N'-tetramethylmethylenediamine (TEMED, Sigma-Aldrich). This solution was mixed by inverting the tube. Then the solution was carefully poured into empty PAGE cassettes (1.5 mm thickness, mini, Thermo Fisher Scientific). The prepared volume was sufficient for four

cassettes. Combs were carefully placed into the cassettes without spilling the solution. The cassettes were incubated for 30 min. For storage the cassettes were placed in a bag with 0.5X TBE buffer and placed at 4 °C until further usage.

Sample Loading Preparation. A 5 μ L sample of the AGE extracted sample were mixed with 5 μ L of 2X denaturing loading solution (50% formamide, 10 mM NaOH, traces of bromophenol blue and xylene cyanol). For the ladder, 1 μ L of 10 bp ladder (Thermo Scientific) were mixed with 0.5 μ L 10X folding buffer, 5 μ L of 2X denaturing loading dye and 3.5 μ L of ultrapure water. The empty lanes were filled with a blank solution composed of 0.5 μ L 10X folding buffer, 5 μ L of 2X loading dye and 4.5 μ L of ultrapure water.

Protocol for Running the Gel. TBE buffer (0.5X) warmed to ~65 °C was used as the running buffer. The lanes were washed with 0.5X TBE buffer using a syringe. The gel was prerun at 220 V for 30 min inside a thermobox filled with hot water (~65 °C). The lanes were washed with 0.5X TBE buffer using a syringe. The prepared samples were loaded into the lanes (10 μ L each). The gel was run under the same condition as in the prerun. After the run, the gel was post-stained with 1X SYBR gold (Life Technologies). The gel staining solution contained a mix of 45 mL of ultrapure water and 5 mL of absolute ethanol. To this mixture 5 μ L of the SYBR gold dye (solution in DMSO) were added. The gel was imaged with a Typhoon FLA 9500 gel scanner (GE Healthcare) using the excitation wavelength of 473 nm, suitable for SYBR gold-stained gels.

tSEM Characterization. Carbon-coated TEM grids (400 mesh copper, carbon on Formvar, Science Services Munich) were plasma-treated for 15 s. A 5 μ L aliquot of the sample solution was applied on the TEM grid and incubated for 3 min. The excess solution was removed from the grid with a filter paper. Next, 5 μ L of a 2% uranyl formate solution were applied for 90 s to stain the DNA origami structures, and the solution was removed with a filter paper. Additionally, two washing steps were performed with ultrapure water for 10 s each, and the water was removed with a filter paper. The samples were scanned on Gemini SEM500 (Zeiss) operated at 30 kV.

AFM Imaging. A 70 μ L sample of a 0.01% poly-L-ornithine solution (Sigma-Aldrich) was placed on a piece of freshly cleaved mica. After 1 min, the mica surface was washed with water; 3 μ L of the respective sample was placed inside a circle (diameter ca. 3 mm) drawn with a permanent marker. After incubation for 1 min, 70 μ L of 1X FB was added to the sample, and 30 μ L of the same buffer was added onto the AFM tip (BioLever-mini, Olympus). Scanning was performed using AC liquid mode using a Cypher ES AFM (Asylum Research).

AGE Based Folding-Yield Estimation. The quantification of the bands on AGE was done using ImageJ (<http://rsb.info.nih.gov/ij/>).

Gibbs Free Energy Simulation Using mfold. mfold is a tool that helps in the prediction of secondary structures of RNA and DNA by using thermodynamics.³⁹ In the current study, this algorithm was used to compute the Gibbs free energy for the gap regions in the two gap designs (small and large). For this purpose, conditions similar to the experiments were chosen (10 mM MgCl₂, 50 mM NaCl) and four different temperatures (12, 25, 37, and 45 °C) were simulated. The output values were plotted on the respective structure design in the form of a heat map graphic with the help of k-router¹⁵ using a color-coded scheme where the results were classified into four categories depending on the computed Gibbs free energy value and the observation from the PAGE analysis (Supporting Figure 17).

ASSOCIATED CONTENT

S Supporting Information

The Supporting Information is available free of charge on the ACS Publications website at DOI: [10.1021/acsnano.7b08345](https://doi.org/10.1021/acsnano.7b08345).

Scaffold designs (ZIP)

Schematics or DNA origami wireframe structures; AGE films; tSEM micrographs; efficiency comparisons; other figures as described in the text (PDF)

AUTHOR INFORMATION

Corresponding Author

*E-mail: Thorsten-Lars.Schmidt@tu-dresden.de.

ORCID

Thorsten L. Schmidt: 0000-0002-6798-5241

Author Contributions

[#]N.P.A. and M.M. contributed equally to this work. M.M., N.P.A., and T.L.S. conceived the study, M.M. designed the structures, N.P.A. and M.M. performed the experiments. N.P.A. performed the tSEM measurements, M.M. performed the AFM imaging, and B.J. helped with the PAGE analysis and quantification. M.M. and N.P.A. wrote the manuscript and prepared the figures.

Funding

This work was funded by the DFG through the Center for Advancing Electronics Dresden (caed), as well as seed Grant 043_2615A6 by the DFG Center for Regenerative Therapies Dresden (CRTD) to T.L.S.

Notes

The authors declare no competing financial interest.

ACKNOWLEDGMENTS

We acknowledge the use of the imaging facilities in the Dresden Center for Nanoanalysis (DCN) and skillful advice from Dr. Markus Löffler, and access to the AFM of Prof. Michael Mertig.

REFERENCES

- (1) Seeman, N. *Structural DNA Nanotechnology*; Cambridge University Press, Cambridge, UK, 2015.
- (2) Jones, M. R.; Seeman, N. C.; Mirkin, C. A. Programmable Materials and the Nature of the DNA Bond. *Science* **2015**, *347*, 1260901.
- (3) Schmidt, T. L.; Heckel, A. Construction of a Structurally Defined Double-Stranded DNA Catenane. *Nano Lett.* **2011**, *11*, 1739–1742.
- (4) Ackermann, D.; Schmidt, T. L.; Hannam, J. S.; Purohit, C. S.; Heckel, A.; Famulok, M. A Double-Stranded DNA Rotaxane. *Nat. Nanotechnol.* **2010**, *5*, 436–442.
- (5) Rothemund, P. W. K. Folding DNA to Create Nanoscale Shapes and Patterns. *Nature* **2006**, *440*, 297–302.
- (6) Douglas, S. M.; Dietz, H.; Liedl, T.; Höglberg, B.; Graf, F.; Shih, W. M. Self-Assembly of DNA into Nanoscale Three-Dimensional Shapes. *Nature* **2009**, *459*, 414–418.
- (7) Dietz, H.; Douglas, S. M.; Shih, W. M. Folding DNA into Twisted and Curved Nanoscale Shapes. *Science* **2009**, *325*, 725–730.
- (8) Hong, F.; Zhang, F.; Liu, Y.; Yan, H. DNA Origami: Scaffolds for Creating Higher Order Structures. *Chem. Rev.* **2017**, *117*, 12584–12640.
- (9) Ke, Y.; Douglas, S. M.; Liu, M.; Sharma, J.; Cheng, A.; Leung, A.; Liu, Y.; Shih, W. M.; Yan, H. Multilayer DNA Origami Packed on a Square Lattice. *J. Am. Chem. Soc.* **2009**, *131*, 15903.
- (10) Ke, Y.; Voigt, N. V.; Gothelf, K. V.; Shih, W. M. Multilayer DNA Origami Packed on Hexagonal and Hybrid Lattices. *J. Am. Chem. Soc.* **2012**, *134*, 1770–1774.
- (11) Han, D.; Pal, S.; Yang, Y.; Jiang, S.; Nangreave, J.; Liu, Y.; Yan, H. DNA Gridiron Nanostructures Based on Four-Arm Junctions. *Science* **2013**, *339*, 1412–1415.
- (12) Simmel, S. S.; Nickels, P. C.; Liedl, T. Wireframe and Tensegrity DNA Nanostructures. *Acc. Chem. Res.* **2014**, *47*, 1691–1699.
- (13) Zhang, F.; Jiang, S.; Wu, S.; Li, Y.; Mao, C.; Liu, Y.; Yan, H. Complex Wireframe DNA Origami Nanostructures with Multi-Arm Junction Vertices. *Nat. Nanotechnol.* **2015**, *10*, 779–784.
- (14) Benson, E.; Mohammed, A.; Gardell, J.; Masich, S.; Czeizler, E.; Orponen, P.; Höglberg, B. DNA Rendering of Polyhedral Meshes at the Nanoscale. *Nature* **2015**, *523*, 441–444.
- (15) Matthies, M.; Agarwal, N. P.; Schmidt, T. L. Design and Synthesis of Triangulated DNA Origami Trusses. *Nano Lett.* **2016**, *16*, 2108–2113.
- (16) Veneziano, R.; Ratanalert, S.; Zhang, K.; Zhang, F.; Yan, H.; Chiu, W.; Bathe, M. Designer Nanoscale DNA Assemblies Programmed from the Top Down. *Science* **2016**, *352*, 1534–1534.
- (17) Liu, Q.; Song, C.; Wang, Z.-G.; Li, N.; Ding, B. Precise Organization of Metal Nanoparticles on DNA Origami Template. *Methods* **2014**, *67*, 205–214.
- (18) Gür, F. N.; Schwarz, F. W.; Ye, J.; Diez, S.; Schmidt, T. L. Toward Self-Assembled Plasmonic Devices: High-Yield Arrangement of Gold Nanoparticles on DNA Origami Templates. *ACS Nano* **2016**, *10*, 5374–5382.
- (19) Agarwal, N. P.; Matthies, M.; Gür, F. N.; Osada, K.; Schmidt, T. L. Block Copolymer Micellization as a Protection Strategy for DNA Origami. *Angew. Chem., Int. Ed.* **2017**, *56*, 5460–5464.
- (20) Marini, M.; Piantanida, L.; Musetti, R.; Bek, A.; Dong, M.; Besenbacher, F.; Lazzarino, M.; Firrao, G. A Reversible, Autonomous, Self-Assembled DNA-Origami Nanoactuator. *Nano Lett.* **2011**, *11*, 5449–5454.
- (21) Zhang, D. Y.; Seelig, G. Dynamic DNA Nanotechnology Using Strand-Displacement Reactions. *Nat. Chem.* **2011**, *3*, 103–113.
- (22) Gonçalves, D. P. N.; Schmidt, T. L.; Koeppl, M. B.; Heckel, A. DNA Minicircles Connected via G-Quadruplex Interaction Modules. *Small* **2010**, *6* (12), 1347–1352.
- (23) Schmidt, T. L.; Koeppl, M. B.; Thevarpadam, J.; Gonçalves, D. P. N.; Heckel, A. A Light Trigger for DNA Nanotechnology. *Small* **2011**, *7* (15), 2163–2167.
- (24) Schmidt, T. L.; Beliveau, B. J.; Uca, Y. O.; Theilmann, M.; Da Cruz, F.; Wu, C.-T.; Shih, W. M. Scalable Amplification of Strand Subsets from Chip-Synthesized Oligonucleotide Libraries. *Nat. Commun.* **2015**, *6*, 8634.
- (25) Niekamp, S.; Blumer, K.; Nafisi, P. M.; Tsui, K.; Garbutt, J.; Douglas, S. M. Folding Complex DNA Nanostructures from Limited Sets of Reusable Sequences. *Nucleic Acids Res.* **2016**, *44*, gkw208.
- (26) Schiffels, D.; Szalai, V. A.; Liddle, J. A. Molecular Precision at Micrometer Length Scales: Hierarchical Assembly of DNA-Protein Nanostructures. *ACS Nano* **2017**, *11*, 6623–6629.
- (27) Lu, X.-J.; Olson, W. K. 3DNA: A Software Package for the Analysis, Rebuilding and Visualization of Three-Dimensional Nucleic Acid Structures. *Nucleic Acids Res.* **2003**, *31*, 5108–5121.
- (28) Wang, J.; Yu, P.; Lin, T. C.; Konigsberg, W. H.; Steitz, T. A. Crystal Structures of an NH₂-Terminal Fragment of T4 DNA Polymerase and Its Complexes with Single-Stranded DNA and with Divalent Metal Ions. *Biochemistry* **1996**, *35*, 8110–8119.
- (29) Erickson, R. O. Tubular Packing of Spheres in Biological Fine Structure. *Science* **1973**, *181*, 705–716.
- (30) Wasserman, S. A.; Cozzarelli, N. R. Determination of the Stereostructure of the Product of Tn3 Resolvase by a General Method. *Proc. Natl. Acad. Sci. U. S. A.* **1985**, *82*, 1079–1083.
- (31) Meyer, M.; Kircher, M. Illumina Sequencing Library Preparation for Highly Multiplexed Target Capture and Sequencing. *Cold Spring Harb. Protoc.* **2010**, *2010*, pdb.prot5448.
- (32) Dale, R. M. K.; McClure, B. A.; Houchins, J. P. A Rapid Single-Stranded Cloning Strategy for Producing a Sequential Series of Overlapping Clones for Use in DNA Sequencing: Application to Sequencing the Corn Mitochondrial 18 S rRNA. *Plasmid* **1985**, *13*, 31–40.
- (33) Cancéll, D.; Viguera, E.; Ehrlich, S. D. Replication Slippage of Different DNA Polymerases Is Inversely Related to Their Strand Displacement Efficiency. *J. Biol. Chem.* **1999**, *274*, 27481–27490.
- (34) Joffroy, B.; Uca, Y. O.; Prešern, D.; Doye, J. P. K.; Schmidt, T. L. Rolling Circle Amplification Shows a Sinusoidal Template Length-Dependent Amplification Bias. *Nucleic Acids Res.* **2018**, *46*, 538–545.
- (35) Zuker, M. Mfold Web Server for Nucleic Acid Folding and Hybridization Prediction. *Nucleic Acids Res.* **2003**, *31*, 3406–3415.
- (36) Jungmann, R.; Liedl, T.; Sobey, T. L.; Shih, W.; Simmel, F. C. Isothermal Assembly of DNA Origami Structures Using Denaturing Agents. *J. Am. Chem. Soc.* **2008**, *130*, 10062–10063.

(37) Sobczak, J.-P. J.; Martin, T. G.; Gerling, T.; Dietz, H. Rapid Folding of DNA into Nanoscale Shapes at Constant Temperature. *Science* **2012**, *338*, 1458–1461.

(38) Liedl, T.; Höglberg, B.; Tytell, J.; Ingber, D. E.; Shih, W. M. Self-Assembly of Three-Dimensional Prestressed Tensegrity Structures from DNA. *Nat. Nanotechnol.* **2010**, *5*, 520–524.

(39) Zuker, M. Mfold Web Server for Nucleic Acid Folding and Hybridization Prediction. *Nucleic Acids Res.* **2003**, *31* (13), 3406–3415.